

# **Abrasive Jet Machining on Soda lime Glass- An experimental investigation**

Dr. D.V. Srikanth<sup>1</sup>, M. Bhojendra Naik<sup>2</sup>, Dr. M. Sreenivasa Rao<sup>3</sup>

<sup>1</sup>Department of Mechanical Engineering, St.Martin's Engineering College, Hyderabad, A.P.India

<sup>2</sup>Department of Mechanical Engineering, St.Martin's Engineering College, Hyderabad, A.P.India

<sup>3</sup>Dept. of Mechanical Engineering, JNTUH, Kukatpally, Hyderabad, A.P. India.

*E-Mail : bhojnaik@gmail.com, dvsk75@gmail.com,*

## **Abstract**

The paper presents an experimental-based study of abrasive jet machining (AJM) considering the effect of changing process parameters. A series of drilling tests were carried out on glass work pieces using sand as the abrasive powder. The influence of each process parameter; applied air pressure, standoff distance, nozzle diameter, particle grain size and impact angle on the machining performance was determined in terms of the resultant material removal rate (MRR). The experimental results revealed that MRR was highly dependent on the kinetic energy of the abrasive particles, with the applied pressure the dominant parameter. The experimental results were compared with an erosion rate model previously published by Jafar et al. Though correct trends were predicted, there was a large discrepancy between model and measured values.

**Keywords:** abrasive jet machining, material removal rate, optimization

## **1. Introduction**

In Jet machining (AJM), an engaged stream of fine grating particles conveyed by profoundly pressurized air strikes the workpiece, and material is expelled from the surface by mechanical disintegration. High weight air (or gas) gives the particles a high speed (high motor vitality) as they leave the spout to affect the workpiece and cause little breaks. The air stream conveys both the rough particles and the cracked material away (Indian Institute of Technology, Kharagpur, 2015; Jagadeesha, 2015; Marinov, 2012).

AJM is a powerful machining technique for hard and fragile materials. Also, notwithstanding its wide applications at the large scale, it has as of late assumed a noteworthy job in small scale machining, particularly miniaturized scale measured highlights, for example, smaller scale directs and smaller scale openings in the production of miniaturized scale gadgets. For a profoundly proficient AJM process, it is important to advance the procedure parameters to build the material evacuation rate (MRR) while acquiring a produced surface of good quality (Jafar, Spelt, and Papini, 2013).

Following this presentation, the paper exhibits and talks about past related work. At that point it depicts the test rig utilized during the examination and the plan of the analyses, trailed by a

discourse of the exploratory outcomes acquired and contrasts these outcomes and the recently created by Jafar et al. (2013). From that point onward, the paper presents the execution of the system pursued by a test preliminary to approve the outcome. At long last, ends are drawn.

## **Related work**

An extensive number of examinations have been completed on AJM both to clarify the different disintegration components and to ponder the elements affecting execution; MRR, dimensional precision, realistic surface quality, and so on.

The weak and malleable disintegration modes have been depicted much of the time in the writing. In fragile break, the material evacuation happens because of the arrangement and proliferation of splits in the work piece material (7. R. Balasubramaniam, J. Krishnan and N.Ramakrishnan (2002)). At the point when the particles sway the workpiece with adequate power, the contact zone is plastically disfigured. Huge pliable anxieties are produced in the objective material that outcome in spiral and parallel break arrangement (8. A. P. Verma and G. K. Lal Publication, 1999; Chen, Hutchinson, and Evans, 2005; Gross, Price, and Glaesemann, 2013; Marshall, Lawn, and Evans, 1982; Wensink, 2002; Wensink, Berenschot, Jansen, and Elwenspoek, 2000). Material evacuation happens when the horizontal break arrives at the surface as appeared in Figure 1 (Wensink, 2002). The volume of splits depends essentially on the mechanical properties of the objective material and the active vitality of the particles (Aquaro, 2010; Bouten et al., 1999; Chen et al., 2005). Greatest disintegration for fragile materials happens at a 90° effect edge, for example the shaft is opposite to the work surface.

The impacts of procedure parameters on the effect disintegration rate when utilizing strong particles have been significant points of research as of late. Sundararajan and Roy (1997) researched the impacts of molecule shape on the disintegration rate. It was discovered that at little effect edges, particles with more precise surfaces caused higher disintegration rates than particles with increasingly adjusted surfaces. Desale, Gandhi, and Jain (2005) revealed that expansion in thickness, hardness and precision of the effect particles caused expanded wear. Desale, Jain, and Gandhi (2009) and other research gatherings (Liebhard and Levy, 1991; Lynn, Wong, and Hector, 1991; Ran et al., 2014) have announced that expanding molecule size prompts bigger and more profound spaces and higher disintegration rates.

Hutchings (1981) directed a trial examination of AJM, estimating disintegration rate for both malleable and fragile materials for various molecule speeds. It was discovered that, every single other factor being equivalent, disintegration rate expanded with expanded molecule speed. Jagadeesha (2015) announced that expanding the standoff separation (SoD) prompts an expansion in disintegration up to a specific worth, after which, the disintegration rate diminishes once more. This is ascribed for the most part with the impact SoD has on the effect speed of particles and their related motor vitality. Wakuda, Yamauchi, and Kanzaki (2002) explored the impact of properties of the workpiece and rough powder while machining clay materials utilizing

AJM. It was discovered that MRR was influenced by break strength and hardness of the objective material, and essentially affected by the kind of grating powder utilized.

Various exploratory examinations on the machining of glass by AJM have been accounted for (Chandra, 2011; El-Domiaty, Abd El-Hafez, and Shaker, 2009; Fan, Wang, and Wang, 2009; Grover, Kumar, and Murtaza, 2014; Kandpal, Kumar, Kumar, Sharma, and Deswal, 2011; Padhy and Nayak, 2014; Sharma and Deol, 2014; Vadgama, Gaikwad, Upadhyay, and Gohil, 2015; Zhang, Kuriyagawa, Yasutomi, and Zhao, 2005). El-Domiaty, et al. (2009) contemplated this issue by directing a progression of boring trials utilizing sand as the rough material with various qualities for different procedure parameters. They found that the MRR expanded with increment in molecule size, applied weight ( $P_r$ ) and spout distance across ( $dn$ ). Chandra (2011) and Kandpal et al. (2011) likewise did test boring of glass by AJM. Their outcomes indicated that as  $P_r$  expanded the MRR expanded. Vadgama et al. (2015) and Padhy and Nayak (2014) utilized the Taguchi technique to configuration tests for penetrating glass by AJM. They likewise found that MRR expanded with the expansion of both  $P_r$  and SoD up to a specific point of confinement after which there was an abatement of MRR. Sharma and Deol (2014) found that the decrease cut and overcut of openings diminished with expanding  $P_r$  and  $dn$ , and diminishing SoD. Grover et al. (2014) consolidated the Taguchi technique and ANOVA to dissect the impact of procedure parameters on AJM and found that MRR diminished with diminishing effect point and rough molecule grain size ( $dg$ ). Fan et al. (2009) created prescient scientific models for the MRR in the miniaturized scale machining of gaps and channels on glasses utilizing AJM. It was discovered that the MRR expanded with the expansion in  $P_r$  and SoD and marginally diminished with the expansion in grating mass stream rate. Zhang et al. (2005) researched miniaturized scale rough discontinuous fly machining for penetrating little openings. This strategy was utilized to guarantee the normal expulsion of the grating particles thus avoid framework blockages.

An audit of the writing shows that the incredible lion's share of distributed work is trial. There exists a genuine absence of research in the region advancement, and this investigation tended to this hole, specifically to upgrade the AJM procedure. In this unique circumstance, this examination incorporated an efficient report to explore the impact of the procedure parameters on the AJM and in this way control them for the most ideal exhibition. The test preliminaries were done under a scope of  $P_r$ , SoD,  $dn$ , and  $dg$ . From that point onward, the outcomes were contrasted and the MRR model distributed as of late by Jafar et al. (2013).

### **Machining setup**

In order to carry out the experimental work, a CNC machine with three axis capability was adapted to enable the fixing of the AJM tool. The machine has a work-table with the following dimensions  $150 \times 250 \times 25$  cm in the  $x$ -,  $y$ - and  $z$ -axes, respectively, with a maximum traverse speed of 120 m/min.

A compressor with a maximum pressure of 10 bar was used to achieve a range of  $P_r$ . Three cylindrical tubes each of length 30 mm and internal diameters 4.0, 5.0 and 6.0 mm were used as

the nozzles for the cutting process, see Figure 2. Sand was chosen as the abrasive material. In order to prepare the sand for the experiment, it was dried and sieved to separate the grains into different sizes. For abrasive sieving, a sieve shaker, with seven sieves was used to obtain three ranges of particle sizes, see Figure 3. The average diameter of the sieved particles in each of the three ranges used in the experimental work were  $150 \pm 50$ ,  $300 \pm 50$  and  $600 \pm 50$   $\mu\text{m}$ .

### Nozzle figures



Fig.1 shows the different sizes of diameter of the Abrasive jet nozzle



Fig. 2 Abrasive jet machining setup

Soda lime glass of 3.0 mm thickness was selected as a target. Using the adjustment holder shown in Figure 4, the blasting gun could be tilted to give suitable impact angles. Figure 5 illustrates the layout of the AJM equipment.

The properties of abrasive (sand) and the workpiece (glass) are as follows (GWP Consultants, 2010); Density of abrasive ( $\rho_p$ ) = 2.316 g/cm<sup>3</sup>, Glass hardness (H) = 5.53 GPa, Glass fracture toughness ( $K_{IC}$ ) = 0.7624 MPa $\sqrt{m}$ , Glass elastic modulus (E) = 71.8 GPa, Glass density ( $\rho_t$ ) = 2.56 g/cm<sup>3</sup>.

Four Process parameters are selected for these experiments

Parameters	Assigned values
Applied air pressure ( $P_r$ )	0.30, 0.60, 0.90 MPa
Standoff distance (SoD)	4.0, 6.0, 10.0 mm
Nozzle diameters ( $d_n$ )	4.0, 5.0, 6.0 mm
Average abrasive grain size ( $d_g$ )	150, 300, 600 $\mu m$

Initial experiments were conducted at an impact angle of 90°. Subsequent tests were carried out at impact angles of 70° and 50° to estimate the effect of impact angle on machining performance. However, it is worth emphasising that prior to commencing the tests, the mass flow rate was measured experimentally at each set of values of the applied process parameters.

### MRR evaluation

MRR can be evaluated by Equation (1); where the weight loss over the test period is divided by the time of the test in minutes.

$$MRR = (w_b - w_a) / t \text{ (g/min)} \text{ -----(1)}$$

where  $w_b$  is the mass of workpiece before the process began,

$w_a$  is the mass of workpiece after the process ended,

and  $t$  is the machining time in minutes. T

The machining time for each trial was the time taken to obtain a hole completely through the test piece. This, of course, varied depending on the given cutting conditions. Each experiment was carried out three times and average value was calculated and presented as the result.

## Results and discussion

Figure , shows test specimens after the drilling process, carried out under different process conditions.

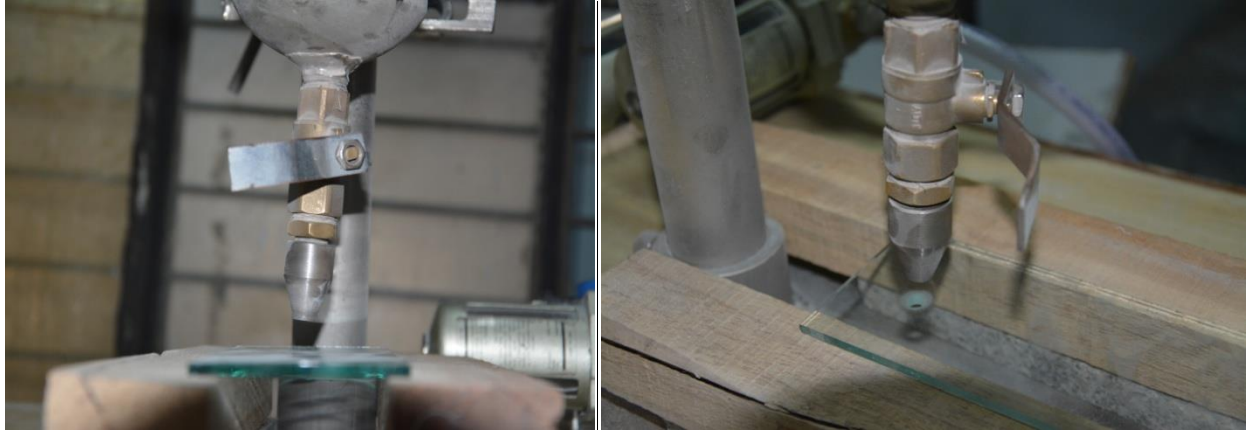


Fig. 3 Glass specimen's setup machining of holes obtained with different process parameters.

### Effect of process parameters on abrasive mass flow rate

Figure (a) and (b) delineates the connection between process parameters ( $P_r$ ,  $d_g$  and  $d_n$ ) and the got mass stream pace of the sand particles. The outcomes exhibited that mass stream rate expanded with the expansion in  $d_n$  at consistent weight, in light of the fact that the bigger spout measurement enables a higher number of particles to exit in a given time. In any case, when  $d_g$  turns out to be moderately huge regarding  $d_n$ , the communication between the particles as they go through the spout gets huge and this cooperation creates a compelling frictional power which diminished the mass stream rate. For instance, it was seen that at least  $d_n$  the bigger the molecule width (of those accessible here) the lower the mass stream rate, see Figure 7(a). At  $d_n = 5.0$  mm, the most noteworthy mass stream rate was seen with  $d_g = 300$   $\mu\text{m}$ . For most extreme spout distance across,  $d_n = 6.0$  mm, the overall estimations of  $d_g$  and  $d_n$  was to such an extent that greatest rough stream was acquired utilizing a grain of size of 600  $\mu\text{m}$  and least grating stream happened with grain size of 150  $\mu\text{m}$ . Apparently the greatest grating mass stream rate for the distinctive molecule sizes is related with utilizing the suitable  $d_n$ .

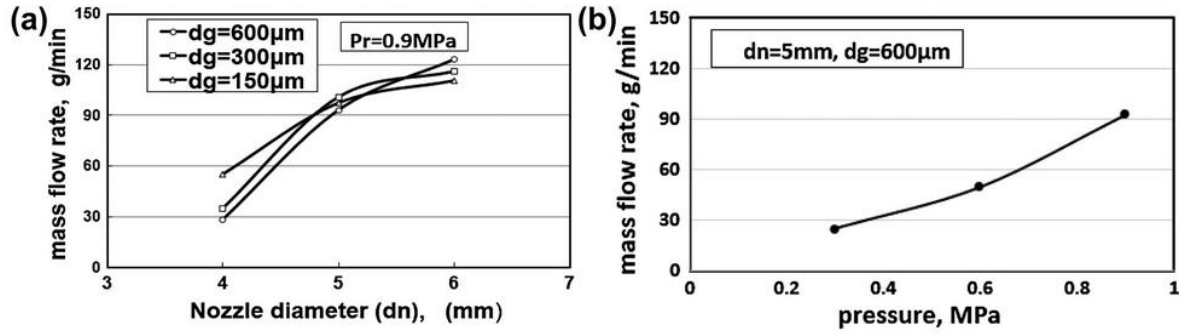


Fig. 4 Effect of process parameters on abrasive mass flow rate; (a) Effect of nozzle diameter on mass flow rate with different particle sizes (b) Effect of air pressure on mass flow rate for  $d_n = 5.0$  mm and  $d_g = 600$  μm.

It was found that  $P_r$  was the most significant parameter influencing the abrasive mass flow rate with mass flow rate increasing monotonically with  $P_r$ . Higher pressure generated higher particle velocity from the nozzle and thus increased the overall mass flow rate.

#### Effect of abrasive particle grain size

The results obtained show that increasing particle grain size generally resulted in an increase in the MRR see Figure. The increase in mass of the abrasive particles resulted in an increase in their kinetic energy and, therefore, the MRR also increased. However, it was observed that use of an appropriate nozzle diameter was required. Figure shows that for the narrowest tube,  $d_n = 4.0$  mm, and lowest air pressure,  $P_r = 0.30$  MPa, this effect is reversed. In these circumstances increasing particle size actually decreases MRR. This is explained as follows; when the  $d_n$  is sufficiently small with respect to  $d_g$ , the flow conditions are such that inter-particle reactions introduce frictional forces that obstruct the flow. It is also known that for small orifices the thermo-viscous effects on the nozzle boundary wall layer can become important and hinder the free flow of air (Förner, Temiz, Polifke, Arteaga, & Hirschberg, 2015). Combined, these effects hinder the flow of the larger particles, especially at lower applied pressures, so the abrasive flow rate decreases and the MRR decreases.





## Fig. Abrasive materials

### Effect of impact angle

Figure presents the relationship between the MRR and impact angle. It was found that the MRR increased with increasing impact angle. This is because the greater the impact angle the greater the component of the velocity perpendicular to the working surface, which causes deeper crack formation and leads to the removal of larger volumes of material (Aquaro, [2010](#)).

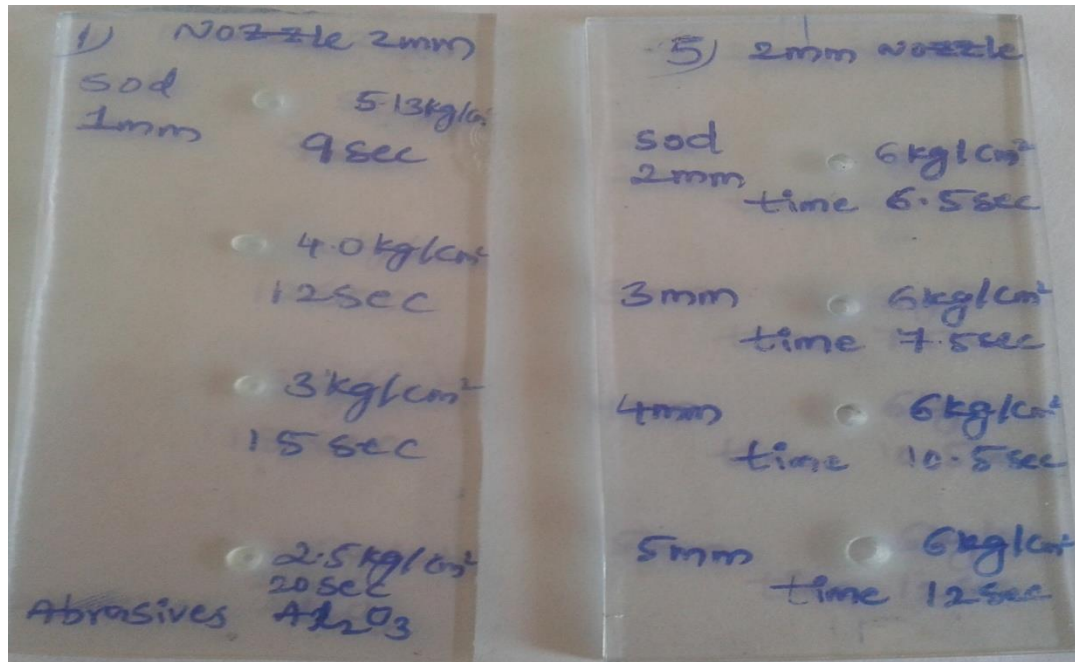


Fig. 4 Effect of impact angle on MRR for glass.

### Effect of nozzle diameter

Figure shows the relationship between nozzle diameter and MRR for different values of  $d_g$ . It was found that when  $d_n$  increased, the MRR also increased, up to a certain limit, after which it decreased. This increase in MRR is because of the increase in flow rate of abrasive particles with larger  $d_n$ , a higher number of particles exit from the nozzle which results in a larger volume of material being removed. This relationship was detected for values of  $d_n$  up to 5.0 mm, above this value, the MRR decreased. This is because the velocity of the particle stream is less at larger  $d_n$  than for a smaller diameter which in turn leads to a reduction in the kinetic energy of the jet and decrease in MRR.

Figure . Effect of nozzle diameter on MRR at different abrasive particle grain size,  $P_r = 0.9$  MPa, SoD = 6.0 mm.



## Effect of standoff distance

Figure (a) and (b) illustrates the relationship between SoD and MRR for different abrasive particle grain size and nozzle pressure. It was found that the MRR increased with increase in SoD up to 6.0 mm, all other parameters constant, but for further increase in SoD the MRR decreased. One can conclude that, in the given circumstances, the optimum value of SoD for maximum MRR was 6.0 mm. The initial increase in MRR is mainly because at small SoDs the inter-collision of particles acts as a frictional force and causes a loss of kinetic energy, and that the small value of SoD makes it difficult for them to move away after impingement as the particles collide with the exit of the nozzle. Moreover, the decrease in MRR for SoD = 6.0 mm is due to a drop in kinetic energy of the particles because of the increase in distance between the exit nozzle and the impact surface (Oh & Cho, 2016).

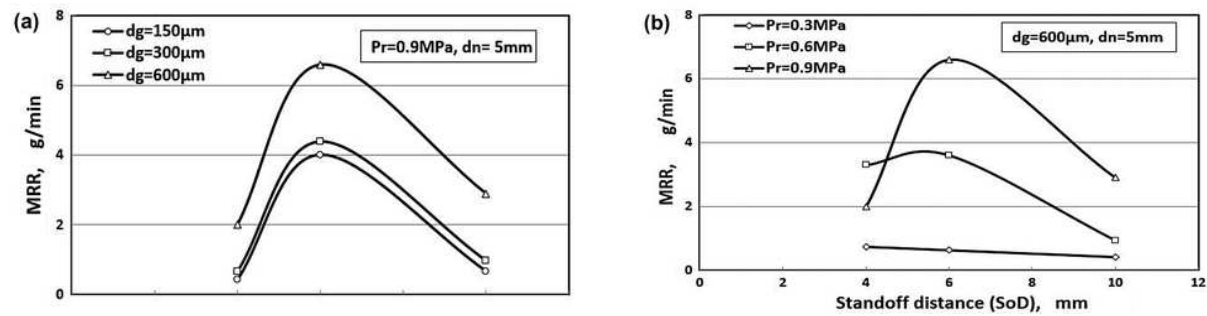


Fig. 5 Effect of standoff distance on MRR (a) with abrasive particle grain size, and (b) with applied pressure.

## Conclusions

In this paper, a detailed study of the AJM has been undertaken that included an experimental investigation, ANN modelling and optimisation of the process parameters governing MRR.

The following are specific conclusions:

- The investigation has demonstrated that MRR increased with increase in the kinetic energy of the abrasive particles.
- It was found that applied pressure was the most significant parameter influencing MRR.
- Nozzle diameter has considerable effect on MRR. For nozzles too small or too large diameter relative to particle size, the MRR decreased.
- The MRR increased with the increase in standoff distance up to a certain limit and then the MRR decreased with the further increase of standoff distance.
- MRR increased with increase in abrasive grain size.
- Highest values of MMR occurred at an impact angle of  $90^\circ$ , oblique impact gave a lower MRR.

## References

- Abdel-Naby, R. (2014). *Effect of abrasive water jet cutting parameters on product quality* (Master thesis). Helwan University, Cairo.  
[\[Google Scholar\]](#)
- Adler, T. (2002). Failure analysis and prevention. *ASM International*, 11, 995–1001.  
[\[Google Scholar\]](#)
- Aquaro, D. (2010). Impact of solid particulate on brittle materials. *Journal of Mechanical Engineering*, 56, 275–283.  
[\[Web of Science ®\]](#), [\[Google Scholar\]](#)
- Aquaro, D., & Fontani, E. (2001). Erosion of ductile and brittle materials. *Meccanica*, 36, 651–661.10.1023/A:1016396719711  
[\[Crossref\]](#), [\[Web of Science ®\]](#), [\[Google Scholar\]](#)
- Bouten, P., Scholten, H., & Pourreux, C. (1999). The strength of glass sheets perforated by erosion. *Wear*, 233-235, 515–522.10.1016/S0043-1648(99)00182-9  
[\[Crossref\]](#), [\[Web of Science ®\]](#), [\[Google Scholar\]](#)
- Chandra, B. (2011). A study of effect of process parameters of abrasive jet machining. *International Journal of Engineering Science and Technology*, 3, 504–513.  
[\[Google Scholar\]](#)
- Chen, X., Hutchinson, J., & Evans, A. (2005). The mechanics of indentation induced lateral cracking. *Journal of the American Ceramic Society*, 88, 1233–1238.10.1111/jace.2005.88.issue-5  
[\[Crossref\]](#), [\[Web of Science ®\]](#), [\[Google Scholar\]](#)
- Desale, G., Gandhi, B., & Jain, S. (2005). Effect of physical properties of solid particle on erosion wear of ductile materials. *World Tribology Congress III Conference in Washington, DC, I*, 149–150.  
[\[Crossref\]](#), [\[Google Scholar\]](#)
- Desale, G., Jain, S., & Gandhi, B. (2009). Particle size effects on the slurry erosion of aluminium alloy (AA 6063). *Wear*, 266, 1066–1071.10.1016/j.wear.2009.01.002  
[\[Crossref\]](#), [\[Web of Science ®\]](#), [\[Google Scholar\]](#)
- El-Domiaty, A., Abd El-Hafez, H., & Shaker, M. (2009). Drilling of glass sheets by abrasive jet machining. *World Academy of Science, Engineering and Technology*, 3, 872–878.  
[\[Google Scholar\]](#)
- Fan, J., Wang, C., & Wang, J. (2009). Modelling the erosion rate in micro abrasive air jet machining of glasses. *Wear*, 266, 968–974.10.1016/j.wear.2008.12.019  
[\[Crossref\]](#), [\[Web of Science ®\]](#), [\[Google Scholar\]](#)
- Finnie, I. (1972). Some observations on the erosion of ductile metals. *Wear*, 19, 81–90.10.1016/0043-1648(72)90444-9

[\[Crossref\]](#), [\[Web of Science ®\]](#), [\[Google Scholar\]](#)

- Förner, K., Temiz, M., Polifke, W., Arteaga, I., & Hirschberg, A. (2015). *On the non-linear influence of the edge geometry on vortex shedding in helmholtz resonators*. Florence: ICSV22, 12–16 July 2015.

[\[Google Scholar\]](#)

- Gross, T., Price, J., & Glaesemann, S. (2013). Sharp contact damage in ion-exchanged cover glass. In *An International Interactive Conference on Functional Glasses: Properties and Applications for Energy & Information*, Siracusa.

[\[Google Scholar\]](#)

- Grover, P., Kumar, S., & Murtaza, Q. (2014). Study of aluminum oxide abrasive on tempered glass in abrasive jet machining using Taguchi method. *International Journal of Advanced Research and Innovation*, 1, 237–241.

[\[Google Scholar\]](#)

- GWP Consultants. (2010). *A study of silica sand quality and end uses in Surrey and Kent, final report for Kent County Council*. Retrieved August 22, 2015, from <http://consult.kent.gov.uk>

[\[Google Scholar\]](#)

- Hutchings, I. (1981). A model for the erosion of metals by spherical particles at normal incidence. *Wear*, 70, 269–281.10.1016/0043-1648(81)90347-1

[\[Crossref\]](#), [\[Web of Science ®\]](#)

, [\[Google Scholar\]](#)